Organic Light-emitting Diodes and Organic Light-emitting Electrochemical Cells Based on Silole-Fluorene Derivatives.

Florian Habrard, T. Ouisse, O. Stephan, Laurent Aubouy, Philippe Gerbier, Lionel Hirsch, Nolwenn Huby, Arie van Der Lee

Organic Light-Emitting Diodes and Organic Light-emitting Electrochemical Cells Based on Silole-Fluorene Derivatives

F. Habrard, T.Ouisse, O.Stéphan

Laboratoire de Spectrométrie Physique (CNRS UMR 5588), Université Joseph Fourier Grenoble I, 140 Rue de la Physique, BP 87, 38402 Saint-Martin d'Hères Cedex, France.

L. Aubouy, Ph. Gerbier

Laboratoire de Chimie Moléculaire et Organisation du Solide (CNRS UMR 5637), Université Montpellier II, CC007, Place Eugène Bataillon, 34095 Montpellier Cedex, France

L. Hirsch, N. Huby

Laboratoire d'Etude de l'Intégration des Composants et Systèmes Electroniques - IXL (CNRS UMR 5818), Université de Bordeaux 1, 351 cours de la Libération, 33405 Talence Cedex, France

A. Van der Lee

Institut Européen des Membranes (CNRS UMR 5635), Université Montpellier II, CC047, Place Eugène Bataillon, 34095 Montpellier Cedex, France

Abstract

Silole groups are known to present a high electron affinity. Initially, copolymerization of siloles with fluorene was aimed at improving electron injection into the polymer layer and so improving the electroluminescent properties of Organic Light Emitting Diodes (OLED's) made from fluorene. But it also provides the ability to turn the light emission colour to the green part of the spectrum and to stop the well known spectral shift degradation occurring in fluorene based materials. In this paper we report the synthesis and the characterisation of 1,1-

dimethyl-2,5-bis(fluoren-2-yl)-3,4-diphenylsilole **4**, and of two soluble conjugated random copolymers derived from 9,9-ditetradecylfluorene and 1,1-dialkyl-2,5-diphenylsilole, where the alkyl group is either methyl **11a** or *n*-hexyl **11b**. Silole **4** crystallizes in the triclinic P_{-1} space group with a = 9.8771(8), b = 10.6240(10), c = 16.585(2) Å, α = 95.775(8), β = 97.025(7), and γ = 111.738(8)°. The results obtained with this molecule, operating in a single-layer OLED (luminance ≈ 450 Cd/m^2 at 12 V; η_{max} = 0.2 Cd/A), give evidences for the complementarity of the silole and the fluorenyl moieties in the improvement of the charge injection processes when compared with 1,1-dimethyl-2,3,4,5-tetraphenylsilole. The results obtained from organic Light Emitting Electrochemical Cells (LEC's) made from silole-fluorene copolymers **11a**, **11b** and molten salts show an improvement of both the device lifetime and the spectral stability when compared with polyfluorene. To explain devices performances electrical characterisation data and Atomic Force Microscope (AFM) imaging were combined.

Keywords: Light-emitting Electrochemical Cells; OLED; Fluorene; Silole; Atomic Force Microscopy

I. Introduction

Organic light emitting devices are expected to replace Liquid Crystal Displays in applications such as mobile phone, digital camera and other devices working with batteries, thanks to a lower energy consumption and inexpensive manufacturing costs. In addition, the possibility to fabricate flexible screens offers the opportunity to create a new range of display devices. However, some drawbacks still have to be overcome in order to reach a commercial performance of a higher standard than competing technologies. For instance, organic devices suffer from a reduced lifetime, often insufficient for commercial applications. Another key point to improve in organic electroluminescent devices is the poor injection balance between holes and electrons. In most conjugated polymers the electron energy barrier between the Fermi level of the metal cathode and the LUMO is higher than the energy barrier for holes at the anode. Besides, using a doped poly(3,4-ethylenedioxythiophene) doped with poly(styrenesulfonate) (PEDOT-PSS) buffer between the transparent indium-tin-oxide (ITO) anode and the active layer still improves hole injection. Hence in a typical ITO/PEDOT-PSS/fluorene/Al structure, the holes mainly contribute to the current, so that only a small fraction of the injected holes can recombined with electrons and give birth to light emission. This behavior is detrimental to devices performances since the weak electron current limits the quantum efficiency. Therefore, the poor injection balance requires the use of a higher operating voltage in order to inject enough electrons so as to obtain an acceptable luminescence level, but leads in turn to a shorter lifetime. Two approaches may be followed to improve the charges balance in fluorene-based devices. The first one involves chemical grafting of electron-transporting groups to the fluorene pattern. Of interest in this perspective are the siloles since they possess high electron acceptability[1, 2] and fast electron mobility.[3] Thereby, interesting results have been already obtained with organic light-emitting diodes and

photovoltaic cells based on silole-fluorene copolymers.[4, 5] The second approach involves the use of Organic Light-emitting Electrochemical Cells (OLEC's) in which the introduction of an ionic salt facilitates both electron and hole injection and induces electro-chemical doping of the active layer.[6-8] Hence OLEC's can be operated at a lower voltage than OLED's. In this paper, we combine both approaches by using silole-fluorene copolymers. Compared with the works already published by Chen et *al.*,[4, 5] we have chosen 2,5-diphenylsiloles instead of 2,3,4,5-tetraphenylsilole since the former are expected to be less prone to emission deactivation induced by the rotation of the phenyl groups attached to the 3,4-positions. The introduction of silole moieties allows one to block the spectral degradation usually observed in fluorene-based conjugated polymers, and to turn the light emission to the green part of the spectrum, in a way quite similar to the use of fluorenone moieties, for which the emission is in the yellow part of the spectrum [9]. More precisely, we have firstly evaluated a silole-fluorene monomer (**4,** figure 1) operating in a single-layer OLED and secondly, we have compared the performance of OLEC's made from two random fluorene-silole copolymers (**11a** and **11b**, figure 3) and from a 9,9'-ditetradecylfluorene homopolymer. To further explain our data we also realized Atomic Force Microscopy (AFM) observations of the silole copolymers / molten salt blends, in a way similar to the one we already described in a previous publication [10].

II. Experimental

II.1. Equipments

Solvents were distilled prior to use. THF and ether were dried over sodium/benzophenone, and distilled under Argon. All the reactions were carried out under argon atmosphere. ^{1}H, ^{13}C and ^{29}Si NMR spectra were recorded on a Bruker Advance 200

DPX spectrometer, the FT-IR spectra on a Thermo Nicolet Avatar 320 spectrometer, the UV-visible spectra on a Secomam Anthelie instrument and the MS spectra on a Jeol JMS-DX 300 spectrometer. I-V characteristics were recorded with a Keithley 2400 Sourcemeter, L-V with a Hamamatsu silicon photodiode placed under the device. Electroluminescence spectra were measured using either an Ocean Optics PC2000 CCD (OLED) or a CVI Spectral Products (OLEC) spectrophotometer. All electroluminescent devices were kept are characterized in a glove box under either nitrogen or argon atmosphere. The synthesis of silole **8a** is described in ref. [11]. AFM images were recorded with a Nanoscope III Dimension 3100 from Veeco Instruments using an Electric Force Microscopy (EFM) mode.[8, 12] In our experiments, we took advantage of the fact that under moderate electric field the polymer is insulating, in contrast with the molten salt domains that are highly polarizable. This allowed us to use the AFM set-up in a Kelvin Probe Force Microscopy mode (KPFM) [13].

II.2. Synthesis

Synthesis of 1,1-dimethyl-2,5-bis(fluoren-2-yl)-3,4-diphenylsilole (4)

A mixture of lithium (0.055 g, 8 mmol) and naphthalene (1.03 g, 8 mmol) in THF (15 mL) was stirred at room temperature under argon for 5 h to form a deep green solution of lithiumnaphthalenide. To the this mixture was added bis(phenylethynyl)dimethylsilane **1** (0.5 g, 2 mmol) in THF (10 mL). After stirring for 10 min, the reaction mixture was cooled to 0° C and [$ZnCl_2$(tmen)] (tmen = *N*,*N*,*N'*,*N'*-tetramethylenediamine) (2.01 g, 8 mmol) was added, followed by an addition of THF (20 mL). After stirring for an hour at room temperature, a solution of 2-bromofluorene **3** (1.176 g, 4.8 mmol) in THF (20mL) and [$PdCl_2(PPh_3)_2$] (0.100 g, 0.13 mmol) were successively added. The mixture was heated under reflux and stirred for 20 h. After hydrolysis by water, the mixture was extracted with Et_2O. After evaporation of the

solvents, the resulting residue was subjected to a silicagel column chromatography CH_2Cl_2/THF (85/15) to give 0.83 g of **4** as a bright yellow solid (70 %). M.p : 271°C. ^{1}H NMR ($CDCl_3$, 25°C): δ = 7.72 (d, $^3J_{HH}$ = 8 Hz, 2H), 7.60 (d, $^3J_{HH}$ = 7 Hz, 2H), 7.48 (d, $^3J_{HH}$ = 7 Hz, 2H), 7.37-7.25 (m, 4H), 7.17 (s, 2H), 7.08-6.95 (m, 8H), 6.90-6.80 (m, 4H), 3.78 (s, 4H), 0.59 (s, 6H). ^{13}C NMR ($CDCl_3$, 25°C): δ = 153.92, 143.33, 143.01, 141.98, 141.71, 139.25, 139.09, 138.66, 130.11, 127.82, 127.49, 126.69, 126.33, 126.19, 125.48, 124.91, 119.63, 119.38, 36.91, -3.47. ^{29}Si NMR ($CDCl_3$, 25°C) : δ = 7.91. MS (EI) *m/z*: 590 [M^+]. Anal calcd for $C_{44}H_{34}Si$: C 89.44, H 5.79; found: C 89.21, H 5.89.

Synthesis of 1,1-dihexyl-2,5-bis(-4-trimethylsilylphenyl)silacyclopentane (6b)

To a suspension of lithium (0.46 g, 66 mmol) in THF (40 mL) was added few drops of a solution of *n*-Hex_2SiCl_2 (5.12 g, 22 mmol) and 4-trimethylsilylstyrene **1** (7.76g, 44 mmol) in THF (10 mL) to initiate the reaction. When the reaction has started, the temperature is lowered to 0°C and maintained through the rest of the addition. After the addition, the reaction mixture is left for 0.5 h at room temperature under stirring, hydrolyzed with a saturated NH_4Cl solution and extracted with ether. The viscous yellow oil, which is obtained upon the evaporation of the solvent, is subjected to a column chromatography (silicagel) to afford 7.51g of **6b** as a colourless viscous oil (62%). ^{1}H NMR ($CDCl_3$, 25°C): δ = 7.49-7.45 (m, 4H), 7.17-7.11 (m, 4H), 2.70-2.16 (m, 6H), 1.57-0.90 (m, 26H), 0.26 (s, 18H). ^{13}C NMR ($CDCl_3$, 25°C): δ = 146.40, 145.46, 135.52, 135.36, 133.75, 126.63, 126.39, 36.57, 34.67, 33.89, 33.76, 32.15, 31.74, 24.63, 23.66, 22.80, 14.53, 14.61, -0.52. ^{29}Si NMR ($CDCl_3$, 25°C): δ = -4.43, 7.00. HRMS (FAB+, m-nitrobenzyl alcohol matrix): *m/z*: calcd for $C_{34}H_{58}Si_3$ [M^+-CH_3] 550.3846; found 550.3821.

Synthesis of 1,1-dihexyl-2,5-bis(4-bromophenyl)silacyclopentane (7b)

To a stirred solution of **6b** (4.0 g, 7.1 mmol) in ether (250 mL) at –80°C was slowly added Br_2 (0.75 mL, 14.5 mmol). After the addition was complete, the temperature is slowly increased to room temperature and left under stirring for 0.5 h. The solvent is then evaporated under vacuum to afford a brown-red semi-solid which is chromatographed on a short silica column to lead to compound **7b** as a pale yellow crystalline solid (2.49 g, 83%). M.p : 82°C. ^{1}H NMR ($CDCl_3$, 25°C): δ = 7.49-7.45 (m, 4H), 7.17-7.11 (m, 4H), 3.11-2.16 (m, 6H), 1.57-0.90 (m, 26H). MS (FAB+, m-nitrobenzyl alcohol matrix) *m/z*: 564 [M^+].

Synthesis of 1,1-dimethyl-2,5-bis(4-bromophenyl)silole (8b)

To a solution of N-Bromosuccinimide (2.09 g, 11.7 mmol) and benzoylperoxyde (10 mg) in CCl_4 (10 mL) heated to reflux was added rapidly **7b** (3.08 g, 5.4 mmol), and then stirred for 1 h. After cooling, the mixture was then filtered and poured into a solution of CH_3CO_2K (1.44 g, 14.7 mmol) and acetic acid (0.1 mL) in acetonitrile (25 mL). The mixture was refluxed for 1h, cooled, hydrolyzed with a saturated NH_4Cl solution and extracted with ether. Evaporation of the solvents yielded a brown-yellow solid that is washed several times with pentane to afford 1.65 g of **8b** as a bright yellow solid (55%). M.p : 166°C. ^{1}H NMR ($CDCl_3$, 25°C): δ = 7.54 (d, $^3J_{HH}$ = 6.5 Hz, 4H), 7.37 (s, 2H), 7.35 (d, $^3J_{HH}$ = 6.5 Hz, 4H), 1.24-0.78 (m, 26H). ^{13}C NMR ($CDCl_3$, 25°C): δ = 143.34, 140.10, 138.72, 132.13, 128.21, 120.85, 33.06, 31.66, 23.87, 22.83, 14.15, 12.33. ^{29}Si NMR ($CDCl_3$, 25°C): δ = 8.42. HRMS (FAB+, m-nitrobenzyl alcohol matrix): *m/z*: calcd for $C_{28}H_{36}Br_2Si$ [M^+] 558.0953; found 558.0975. Anal calcd for $C_{28}H_{36}Br_2Si$: C 60.00, H 6.47; found: C 59.75, H 6.61.

II.3. X-ray structure determination

Experimental and crystal data for **4** ($C_{44}H_{34}Si$). Spearhead single crystals of approximate dimensions 0.15 x 0.08 x 0.08 mm^3 were selected on polarized microscope and mounted on a Bruker-Nonius χ-CCD diffractometer, Mo-K_α radiation (0.71073 Å). Data collection was performed using mixed ϕ and ω scans, 179 frames of 1.5°, 285 seconds per frame and a distance crystal-detector of 30 mm. The structural determination by direct methods and the refinement of atomic parameters based on full-matrix least squares on F^2 were performed using the SHELX-97[15] programs within the WINGX package.[16] Results: a = 9.8771(8) Å, b = 10.6240(10) Å, c = 16.585(2) Å, α = 95.775(8)°, β = 111.738(8)°, γ = 65.70(2), V = 1584.2(3) $Å^3$, density(calc.) = 1.239, triclinic P-1, 87% completeness to theta 32.33°, 11295 collected data, 9879 independent reflections (R_{int}=0.0865) for 1174 refined parameters, R_{obs}=0.087, wR^2_{obs}=0.0805, $(\Delta/\sigma)_{max}$=0.001, largest difference peak and hole 0.46/-0.42 $e.A^{-3}$, max. CCDC - 621990 contains the supplementary crystallographic data for this paper. These data can be obtained free of charge from The Cambridge Crystallographic Data Centre via www.ccdc.cam.ac.uk/datarequest/cif.

II.4. Device fabrication

II.4.1. OLED

EL devices based on silole **4** as both emitting and transporting layer were fabricated, on an ITO substrate covered with a 60 nm-thick layer of PEDOT-PSS deposited by the usual spin-coating techniques and cured at 80 ° for about 1 hour. A 50 nm-thick silole layer was then thermally evaporated under secondary vacuum (around 10^{-6} mbar). The calcium cathode

was evaporated through a shadow mask on top of the silole and capped with a layer of aluminum to minimize its oxidation.

II.4.2. OLEC

In OLEC's, the thickness of the PEDOT-PSS layer deposited onto the ITO anode was about 100 nm. This layer was dried under vacuum at 150°C for 15 mn. After cooling, the active layer was deposited by spin-coating at 1000 rpm using chloroform as a solvent. The active layer of OLEC was constituted of a blend of polymer (20 g/L) and tetrahexylammoniumbis(trifluoromethylsulfonyl)imide (THA-TFSI) ionic liquid (10 g/L) [14]. Then a 150 nm thick aluminum cathode was deposited by metallization under secondary vacuum (under 10^{-6} mbar) through a shadow mask.

III. Results and discussion

III.1. Synthesis

Silole **4** was conveniently prepared by the method described by Tamao *et al.* [1] that involves the one-pot reductive intramolecular cyclization of bis(phenylethynyl)silane **1** and subsequent Pd(0)-catalyzed cross-coupling reaction with 2-bromofluorene **3** as depicted in Figure 1.

The synthesis of siloles **8a** and **8b** is described in figure 2. It involves the synthesis of silacyclopentadienes **6a** and **6b** that was achieved by reacting 4-(trimethylsilyl)styrene **5** with lithium in presence of dimethyldichlorosilane. The trimethylsilyl side-groups was readily and selectively replaced by bromine to yield the bis 4-bromophenyl derivatives **7a** and **7b**. Only Me_3Si-C bond cleavage occurred and no product arising from the cleavage of the ring Si-C

bonds was obtained. Treatment of **7a** or **7b** by two equivalents of *N*-bromosuccinimide in presence of benzoylperoxide, followed by refluxing the mixture in the presence of a weak base yields the siloles **8a** and **8b**, respectively.

Polymers and copolymers were synthesized using the well-known dihalogenative polycondensation of the dibromo monomer or comonomers catalyzed by the bis(1,5-cyclooctadiene)Ni(0) catalyst in a dimethylformamide/toluene mixture as previously described [17]. For copolymers, fluorene (2,7–dibromo-9,9-n-di-tetradecanefluorene) and dibromo silole (**8a** or **8b**) molar feed ratio were 90:10 . In all cases, after precipitation in an acetone/HCl/methanol solution (1:1:1 volume ratio) the crude products were carefully purified by soxhlet extraction using methanol and acetone successively in order to remove residual catalyst and low molecular weight oligomers.

III.2. X-ray structure description

Silole **4** crystallizes in the P_{-1} triclinic space group with a = 9.8771(8), b = 10.6240(10), c = 16.585(2) Å, α = 95.775(8), β = 97.025(7), and γ = 111.738(8)°. Its ORTEP view is presented in Figure 4. The silole displays a propeller-like arrangement of the four aryl groups as usually observed with the others tetraarylsiloles. The dihedral angles between the mean plane of the central silole and the fluorenyl groups have values of 72.7(1)° and 27.8(1)°. As shown in Figure 5, two molecules are associated through the most twisted fluorenyl side-group in inverted head-to-tail dimers by two C(11)-H(56)···π (2.85 Å on average) and two C(14)-H(59)···π (2.73 Å on average) interactions. These dimers are associated in their turn in infinite supramolecular chains[18] along the a^* direction through interactions between the less twisted fluorenyl side-group of a dimer and the silole moiety of another dimer (C(27)-H(66)···π : 2.88 Å and C(20)-H(61)···π : 2.65 Å).

III.3. Photophysical properties

III.3.1. Absorption and photoluminescence spectra

*III.3.1.1. Silole **4***

UV-visible absorption and fluorescence spectra of silole **4** have been measured in diluted solution (Figure 6). The absorption spectrum is characterized by the presence of three intense absorption bands centered at 280, 319 and 392, respectively. The two first bands originate from π-π* transitions of both the fluorenyl moieties and the aryl groups, whereas the last one is characteristic of π-π* transitions involving the silole ring.[11] The photoluminescent properties where investigated using two different excitation wavelengths. When excited at 400 nm, the emission spectrum shows a broad peak centered at *ca.* 519 nm (Φ_{em} = 0.0015), which is characteristic of the silole emission. These values have to be compared with those reported for 1,1-dimethyl-2,3,4,5-tetraphenyl silole (absorption: λ_{max} = 359 nm, emission: λ_{max} = 467 nm, Φ_{em} = 0.0014).[1] The red-shift that is observed for **4** both in absorption and emission is indicative of a substantial perturbation of the HOMO-LUMO levels provided by the presence of the terminal fluorenyl groups. However, the attachment of fluorene to the tetraphenylsilole did not afford any modification of the PL quantum yield that remains very low. In the solid state (thin film), the spectrum (Figure 6) shows only the intense absorption due to the π-π* transitions of the silole ring that is red-shifted of 30 nm (λ_{max} = 549 nm) when compared with the one observed in solution. This difference may be due to the fact that silole **4** adopts different conformations when it is either in solution or in the solid state.

*III.3.1.2. Copolymers **11a** and **11b***

In figure 7 we present absorption spectra of **11a** and **11b** and of the fluorene homopolymer. The three polymers were dissolved in chloroform at a concentration of 5.10^{-2} g/L. Fluorene homopolymer exhibits absorption maximum at 385 nm due to π - π^* transition. Copolymers **11a** and **11b** show similar spectra to fluorene one with the same absorption maximum wavelength but spectra are broader with absorption edges shifted to longer wavelength. This behavior is consistent with results obtain by Wang et al. [19]. For low silole segments content they do not observe any change in absorption maximum wavelength compared with fluorene homopolymer but they observe a quite similar absorption edge shift toward lower energies.

The part of the absorption spectra of the copolymers between 420 and 485 nm is characteristic of the presence of silole moieties that absorb at a smaller energy [20]. If one compare the intensity I_{475nm} / I_{420nm}, one can remark that this ratio is superior for silole with hexyl chains. This can mean that this copolymer has a higher content of silole moieties than the one with methyl chains.

Normalized photoluminescence spectra of the thin solid film made by spin-coating of 10 g/L chloroform solutions of silole-fluorene copolymer **11a** and **11b** onto glass substrates are shown in figure 8. For comparison, thin film PL spectra of fluorene and 2,5-diphenylsilole homopolymers made in the same conditions are also shown in this figure. First of all, it is worthy to note that silole **4** (Figure 6) as well as all the silole-containing polymers display comparable spectra with emission maxima at *ca.* 550 nm, no emission reminiscent from the

fluorene homopolymer is noticed. Secondly, as expected, Förster energy transfer from the higher-energy fluorene segments to the lower-energy silole segments occurs, modifying the color emission from blue to green. [4, 20] Hence silole moieties act as efficient traps for excitons. Another alteration of the properties afforded by the presence of siloles is found in the PL efficiencies: silole copolymers emit more weakly than polyfluorene by a factor ranging from 3.75 (silole methyl) to 7 (silole hexyl). This phenomenon, that have been observed in a less extend with tetraphenyl-based silole-fluorene copolymers, originates from the fact that the energy is transferred to a poorly emissive molecule. In addition, we can see that the copolymer with hexyl chains on the Si atom **11b** emits less than the copolymer with methyl chains **11a**. This difference may be explained by the aggregation-induced emission (AIE) phenomenon that has been observed with the siloles.[21] Therefore, the steric hindrance caused by hexyl chains being less favorable to aggregation, may reasonably explain the weaker emission in the silole hexyl case.

III.3.2. Electroluminescence

*III.3.2.1. Silole **4** operating in OLED's*

Electroluminescent ITO/PEDOT-PSS/silole/Ca devices based on siloles **4** were fabricated. A 50 nm-thick silole layer was then thermally evaporated and calcium was used as the cathode since its work function (2.9 eV) is close to the electron affinity of the siloles.[11] The normalized EL spectrum, that is superimposable to the solid-state PL one, shows also an unique emission peak in the yellow-green region at 550 nm. To evaluate the performance, we examined the current density-voltage (J-V) and luminance-voltage (L-V) characteristics of the devices (Figure 9). Above a threshold voltage of 5.1 V a significant current flows, giving rise

to light emission with a luminance of *ca.* 450 Cd/m^2 at 12 V and a maximum efficiency of 0.2 Cd/A. When compared with the values reported for the closely related 1-methyl-1,2,3,4,5-pentaphenylsilole, operating in a ITO/TPD/silole/Alq_3/Al device[22] (turn-on voltage: 11 V, luminance: *ca.* 80 Cd/m^2 at 12 V, 4538 Cd/m^2 at 18 V), it seems obvious that the replacement of the phenyl side-groups by more efficient hole-transporting fluorenyl groups improves dramatically the efficiency of the devices. Indeed, the approach consisting in the correction of the charge balance by linking in a same molecule fluorene and silole moieties allows a better improvement of the device properties than the use of hole- and electron-transporting layers do.

*III.3.2.2. Copolymers **11a** and **11b** operating in OLEC's*

Figure 10 show the time-dependent electroluminescence (EL) spectra obtained from OLEC's made with the copolymers **11a** or **11b** under stresses of 6 and 8V, respectively. Spectra show only the emission originating from the silole at *ca.* 500 nm as observed with silole **4**. More interesting is that, when compared with the spectra recorded with polyfluorene that experiences a large spectral shift, the silole copolymers show a great stability of the emission wavelength[23-25]. In the case of polyfluorene, the spectral degradation of the emitted light versus stress time is very fast. Initially, EL spectra of fluorene exhibit a peak at 425 nm, with some vibrational replica at longer wavelengths. But rapidly, a strong emission band appears near 550 nm, due to the oxidation of fluorene chains. This oxidation turns the color emission from blue to yellow. The origin of this stability may be explained by the fact that there is a trade of excitons from the fluorene to the silole moieties, where the radiative recombination takes place. We do not observe the effect of fluorene oxidation on the shape of

the EL spectrum. On the other hand, the drop of electroluminescence is rather fast, as for polyfluorene OLEC's, and the origin of the EL intensity degradation is discussed in the next paragraphs.

Figure 11 compares the current-voltage (I-V) and electroluminescence intensity-voltage (L-V) characteristics of OLEC's made either from silole-fluorene copolymers or from the fluorene homopolymer. At first glance, the copolymers **11a** and **11b** exhibit a similar behavior to the one observed with silole **4** operating in the single-layer OLED. However, some differences appear when the comparison is done with the fluorene homopolymer. Indeed, the current level is larger at low voltage with **11a** and **11b** than with the fluorene homopolymer, and the current threshold voltage is lower than that of fluorene. So electrical performance seems to be improved in comparison with fluorene. However we can see that even if the current threshold is greater for the homopolymer than for the copolymers, electroluminescence takes place at a lower voltage. Moreover it is obvious that the EL intensity level of the two copolymers is much weaker than for fluorene (see Figure 11). The luminescence level is 1 or 2 order of magnitude greater for fluorene than for silole copolymers. This result is qualitatively consistent with the photoluminescence data obtained from the same polymers, but quantitatively, the luminescence intensity factor between the copolymers and fluorene is lower for PL than for EL. From Figure 8 it might be inferred that both copolymers are indeed substantially worse than the homopolymer for producing electroluminescence. However, it must be taken into account that such devices require some time to emit light, due to the fact that the electrolyte double-layer formation is not instantaneous [26]. If the molten salt polymer blend is not mixed in the same way, different devices may exhibit quite different current transients. Hence for a more rigorous comparison

it is better to study the variation of current and light emission as a function of time, as achieved in Figure 12, which presents current and EL intensity versus time for the three polymers.

Figure 12 clearly shows that the lifetime of the device made from the copolymer with methyl groups **11a** is much longer than with the fluorene homopolymer. The difference actually observed from the I-V characteristics in Figure 11 simply results from the fact that the maximum of current is obtained after 100s in the case of polyfluorene, and after 40mn in the case of the copolymer with methyl groups. The total amount of emitted light after a 15000s stress at 6V in the case of the copolymer with methyl groups exceeds the light emitted from the device made from the homopolymer by almost a factor of 10. The aging of our OLEC's can be attributed to a degradation of the conjugated polymer around the molten salt domains [10]. Hence it is likely that the copolymer is more resistant than the homopolymer against current-induced degradation. It is worth noticing that the better performance of the silole-fluorene copolymer is obtained with **11a**. As seen in Figure 12, the polymer **11b** answers as rapidly as the homopolymer, but suffers form a reduced current and light emission and premature electrical aging (in Figure 12 the light emission peak is almost undistinguishable from the y axis with the chosen scale). It is worth noticing that the ratio of the total amount of emitted photons over the total amount of injected charge is about the same, both for the homopolymer and the copolymer with methyl side groups. Hence the better performance of the copolymer is due to a better current injection, and not to a better quantum yield.

III.3.3. AFM studies

AFM imaging was used to assess the quality of the ionic liquid-conjugated polymer blends. [10] Typical images of the copolymer/molten salt blends (Figure 13) show that the ionic liquid micro-domains exhibit a disc-like shape. The most favorable blends are characterized by smaller salt domains in the polymer matrix. In the case of copolymers, the salt domains are bigger than for the blend with polyfluorene, so that the difference in current level between the homopolymer and the copolymers cannot be explained by the quality of the blend at the sub-micrometer scale. However, it is also clear that the blend obtained with the copolymer **11a** is much better than the one obtained with the polymer **11b**. Hence the AFM imaging is in agreement with the difference in performance between the two copolymers. But it cannot explain the fact that **11a** permits to obtain almost ten times more emitted photons over the whole device lifetime. It is thus tempting to attribute the better performance of the copolymer to its microscopic properties. For instance, if the injected electrons lie essentially in the silole chains, one can make the assumption that the usual oxidation of the fluorene segments is slower than in the case of the homopolymer, hence the lifetime could be increased.

IV. Conclusion

To improve the characteristics of polyfluorene-based light-emitting devices by correcting the injection balance, we have followed a combined approach consisting in the chemical grafting of electron-transporting groups to the fluorene pattern, operating in an organic light-emitting electrochemical cell (OLEC). In the present case, silole were chosen since they exhibit high electron acceptability and fast electron mobility. To validate this approach, we firstly synthesized silole **4** that is substituted by two fluorenyl groups at its 2,5-

position. The use of **4** as the active layer in a ITO/PEDOT/silole/Ca device allowed us to obtain quite decent performances of *ca.* 450 Cd/m^2 at 12 V with a maximum efficiency of 0.2 Cd/A. It is worthy to note that these values are far above the one obtained with other tetraphenylsilole derivatives, showing therefore the validity of this approach. Pursuing our progress, we have then synthesized two 2,5-diphenylsilole – 9,9'-ditetradecyfluorene copolymers differing by the nature of the organic groups attached to the silicon atom. Compared with the works already published by Chen et *al.*, we have chosen 2,5-diphenylsiloles instead of 2,3,4,5-tetraphenylsilole since the former are expected to be less prone to emission deactivation induced by the rotation of the phenyl groups attached to the 3,4-positions. Our data show that both the PL intensity and EL efficiency of silole-fluorene copolymers in OLEC devices are much weaker than those of fluorene homopolymer, due to intrinsic properties of the silole groups, but nevertheless, higher than those reported for tertraphenylsilole/fluorene copolymers operating in OLED's. Moreover, we have evidenced that the incorporation of siloles motives in the polyfluorene chains affords an appreciable improvement of the spectral stability, thanks to the trade of excitons from the fluorene to the silole moieties. Besides, although OLEC's made from the copolymer with methyl side groups exhibit a delayed performance with respect to devices produced from the fluorene homopolymer, they also exhibit a one order of magnitude lifetime improvement. This would make such devices potentially interesting for applications, provided that the quality of the blend is improved so as to reduce the current transients.

V. Acknowledgments

The authors thank the French CNRS and Région Languedoc-Roussillon for their financial support as well as J. Chevrier (Laboratoire d'Etudes des Propriétés Electronique des Solides and European Synchrotron Radiation Facility) for making available his AFM apparatus.

References

[1] S. Yamaguchi, T. Endo, M. Uchida, T. Izumizawa, K. Furukawa, K. Tamao, *Chem. Eur. J.* **2000**, *6*, 1683.

[2] S. Yamaguchi, K. Tamao, *J. Chem. Soc., Dalton Trans.* **1998**, 3693.

[3] K. Tamao, M. Uchida, T. Izumizawa, K. Furukawa, S. Yamaguchi, *J. Am. Chem. Soc.* **1996**, *118*, 11974.

[4] F. Wang, J. Luo, J. Chen, F. Huang, Y. Cao, *Polymer* **2005**, *46*, 8422.

[5] F. Wang, J. Luo, K. Yang, J. Chen, F. Huang, Y. Cao, *Macromolecules* **2005**, *38*, 2253.

[6] J. A. Manzanares, H. Reiss, A. J. Heeger, *J. Phys. Chem. B* **1998**, *102*, 4327.

[7] Q. Pei, Y. Yang, G. Yu, C. Zhang, A. J. Heeger, *J. Am. Chem. Soc.* **1996**, *118*, 3922.

[8] C. Yang, Q. Sun, J. Qiao, Y. Li, *J. Phys. Chem. B* **2003**, *107*, 12981.

[9] S. Panozzo, J.-C. Vial, Y. Kervella, O. Stephan, *J. Appl. Phys.* **2002**, *92*, 3495.

[10] F. Habrard, T. Ouisse, O. Stephan, M. Armand, M. Stark, S. Huant, E. Dubard, J. Chevrier, *J. Appl. Phys.* **2004**, *96*, 7219.

[11] L. Aubouy, P. Gerbier, N. Huby, G. Wantz, L. Vignau, L. Hirsch, J.-M. Janot, *N. J. Chem.* **2004**, *28*, 1086.

[12] F. P. Wenzl, C. Suess, A. Haase, P. Poelt, D. Somitsch, P. Knoll, U. Scherf, G. Leising, *Thin Solid Films* **2003**, *433*, 263.

[13] H. O. Jacobs, H. F. Knapp, A. R. o. S. I. Stemmer, *Rev. Sci. Instrum.* **1999**, *70*, 1756.

[14] S. Panozzo, M. Armand, O. Stephan, *Appl. Phys. Lett.* **2002**, *80*, 679.

[15] G. M. Sheldrick, Release 97-2 ed., Institüt für Anorganische Chemie der Universität, Tammanstrasse 4, D-3400 Göttingen, Germany, **1998**.

[16] L. J. Farrugia, *J. Appl. Cryst.* **1999**, *32*, 837.

[17] G. Klärner, M.H. Davey, W.D. Chen, J.C. Scott and R.D. Miller, Adv. Mater., **1998**, 10, 993.

[18] D. R. Desiraju, *Chem. Commun.* **2005**, 2995.

[19] F. Wang, J. Luo, J. Chen, F. Huang, Y. Cao, *Polymer*, **2005**, 46, 8422.

[20] M. S. Liu, J. Luo, A. K.-Y. Jen, *Chem. Mater.* **2003**, *15*, 3496.

[21] J. W. Y. Lam, J. Chen, C. C. W. Law, H. Peng, Z. Xie, K. K. L. Cheuk, H. S. Kwok, B. Z. Tang, *Macromol. Symp.* **2003**, *196*, 289.

[22] B. Z. Tang, X. Zang, G. Yu, P. P. S. Lee, Y. Liu, D. Zhu, *J. Mater. Chem.* **2001**, *11*, 2974.

[23] T. Ouisse, O. Stephan, M. Armand, *Eur. Phys. J. Appl. Phys.* **2003**, *24*, 195.

[24] X. Gong, P. K. Iyer, D. Moses, G. C. Bazan, A. J. Heeger, S. S. Xiao, *Adv. Funct. Mater.* **2003**, *13*, 325.

[25] K.-H. Weinfurtner, H. Fujikawa, S. Tokito, Y. Taga, *J. Appl. Phys.* **2000**, *76*, 2502.

[26] T. Ouisse, O. Stephan, M. Armand, J. C. Lepretre, *J. Appl. Phys.* **2002**, *92*, 2795.

Figure captions

Figure 1. Synthesis of silole **4** : (**i**) NpLi; (**ii**) $ZnCl_2$.TMEDA ; (**iii**) $PdCl_2(PPh_3)_2$.

Figure 2. (**i**) Li, Me_2SiCl_2 ; (**ii**) Br_2 ; (**iii**) NBS, benzoyl peroxide ; (**iv**) AcOK/AcOH.

Figure 3. Schematic route for the copolymers synthesis

Figure 4. ORTEP view of the molecular structure of silole **4** (thermal ellipsoids set at 50% of probability)

Figure 5. Side view of the infinite supramolecular chains in the *a** direction, showing short contacts (black dashed lines).

Figure 6. Normalized absorption (—), and photoluminescence (excitation wavelength: 400 nm) spectra of silole **4**, in solution (-•-), and as thin solid film (- -).

Figure 7. Absorption spectra of silole copolymers **11a** and **11b**, and fluorene homopolymer.

Figure 8. Photoluminescence spectra of fluorene and silole homopolymers and of the silole copolymers **11a** and **11b** as thin solid films (excitation wavelength: 365 nm).

Figure 9. Current density-voltage (J-V) and luminance-voltage (L-V) characteristics of ITO/PEDOT/silole/Ca devices based on silole **4**.

Figure 10. Electroluminescence spectra of OLEC (copolymer **11a**, **11b**: 20 g/L; THA-TFSI: 10 g/L) with increasing stress time.

Figure 11. Current and Luminescence versus voltage for fluorene homopolymer and the silole copolymers **11a** and **11b** mixed with THA-TFSI

Figure 12. Current (a) and luminescence (b) versus time for fluorene homopolymer (dotted line), **11b** (dashed line) and **11a** (solid line), blended with THA-TFSI. $C_{polymer}$=20 g/L, $C_{THA\text{-}TFSI}$=10 g/L. Voltage bias is 6 V.

Figure 13. KFM images of **11a** – THA-TFSI (a.) and **11b** – THA-TFSI (b.) blends. EFM image of polyfluorene –THA-TFSI blend (c.)

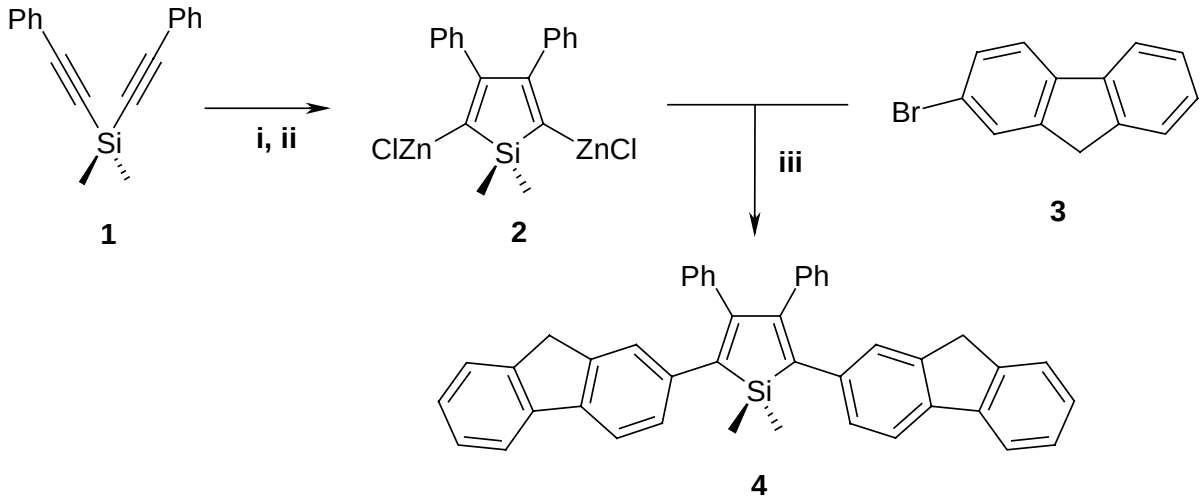

Figure 1

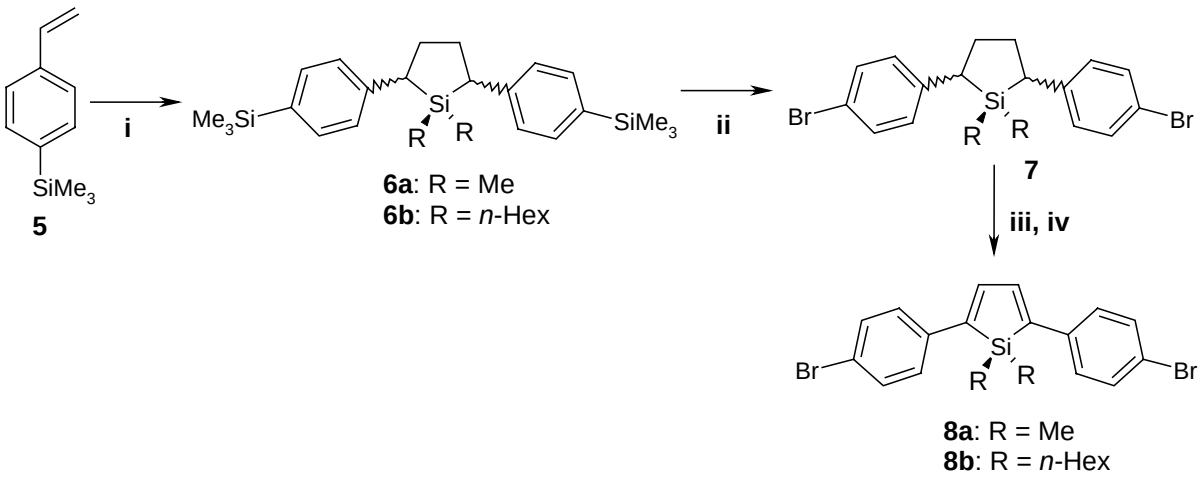
SiMe3
5
i
Me3Si
Si
R
R
SiMe3
6a: R = Me
6b: R = n-Hex
ii
Br
Si
R
R
Br
7
iii, iv
Br
Si
R
R
Br
8a: R = Me
8b: R = n-Hex

Figure 2

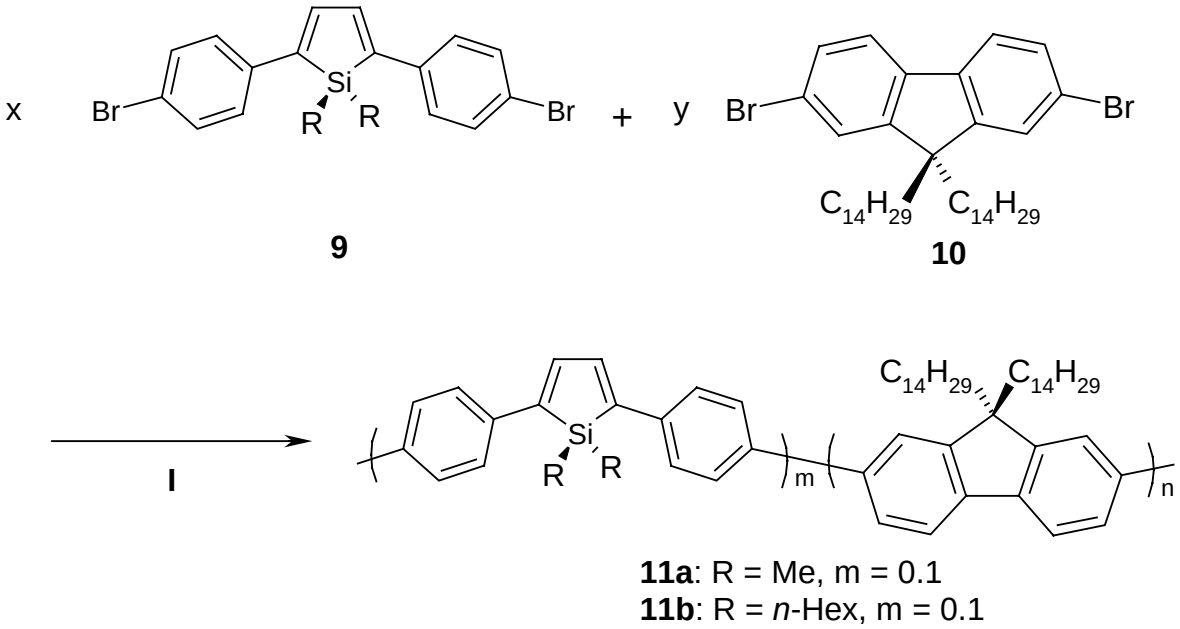
x
Br
Si
R
R
Br
+
y
Br
Br
C14H29
C14H29
9
10
I
C14H29
C14H29
Si
R
R
m
n
11a: R = Me, m = 0.1
11b: R = n-Hex, m = 0.1

Figure 3

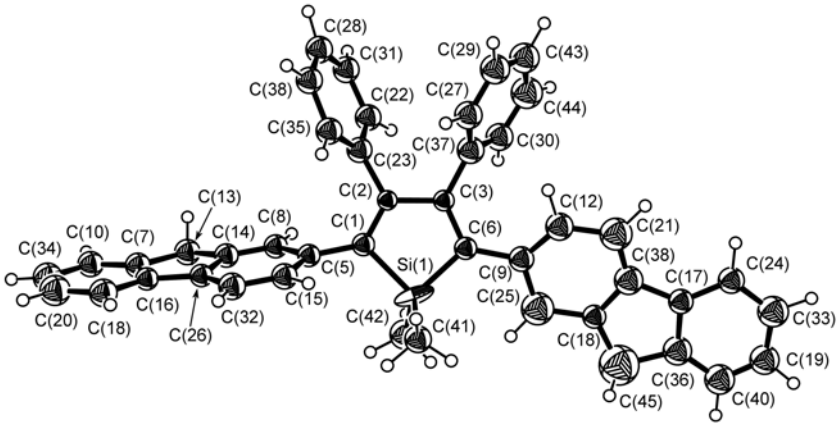
C(28)
C(31)
C(29)
C(43)
C(38)
C(22)
C(27)
C(44)
C(35)
C(37)
C(30)
C(23)
C(2)
C(3)
C(13)
C(12)
C(8)
C(1)
C(6)
C(21)
C(10)
C(7)
C(14)
C(34)
C(5)
Si(1)
C(9)
C(38)
C(17)
C(24)
C(25)
C(16)
C(15)
C(42)
C(41)
C(33)
C(20)
C(18)
C(26)
C(32)
C(18)
C(19)
C(36)
C(45)
C(40)

Figure 4

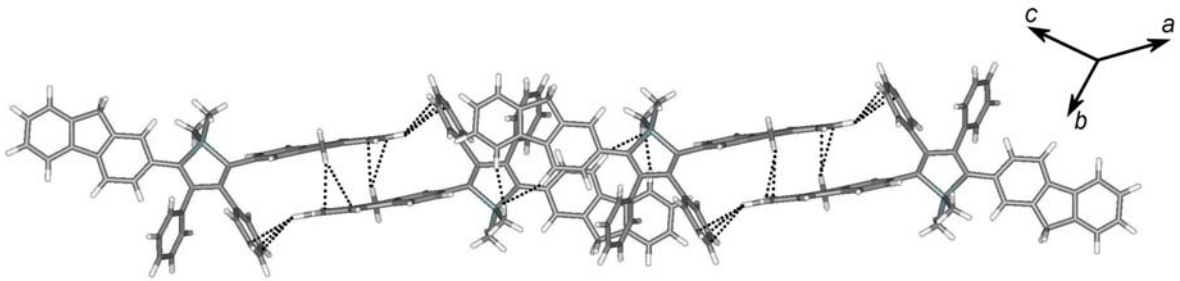

Figure 5

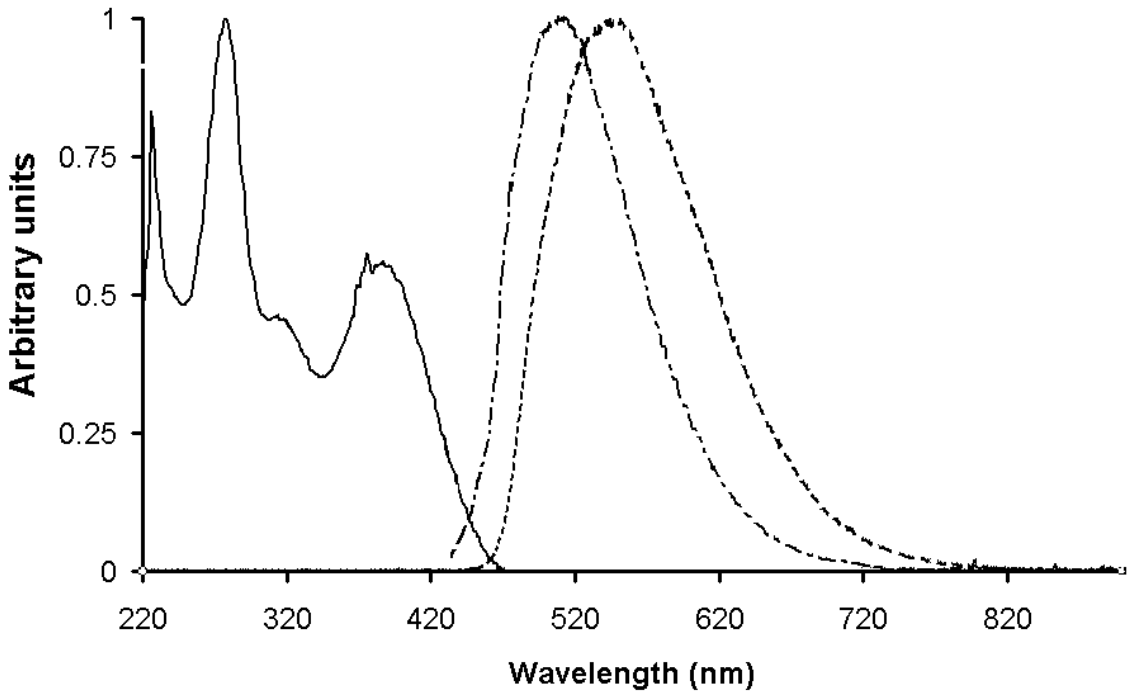
Arbitrary units
1
0.75
0.5
0.25
0
220
320
420
520
620
720
820
Wavelength (nm)

Figure 6

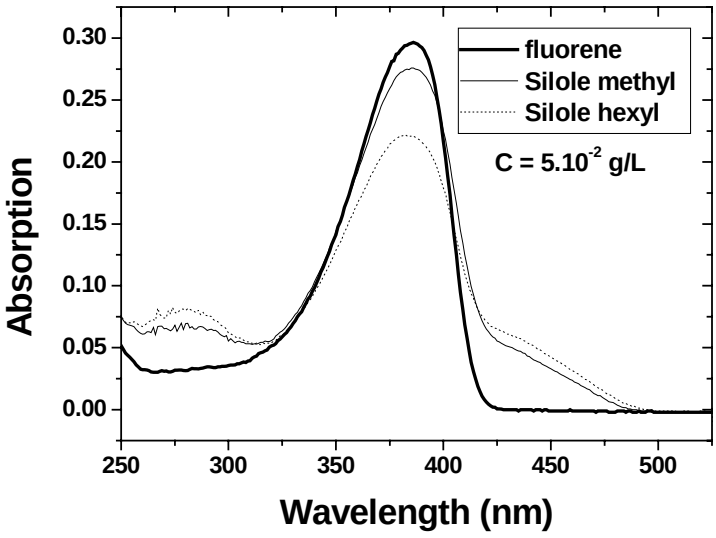
fluorene
Silole methyl
Silole hexyl
C = 5.10-2 g/L
Absorption
Wavelength (nm)
0.00
0.05
0.10
0.15
0.20
0.25
0.30
250
300
350
400
450
500

Figure 7

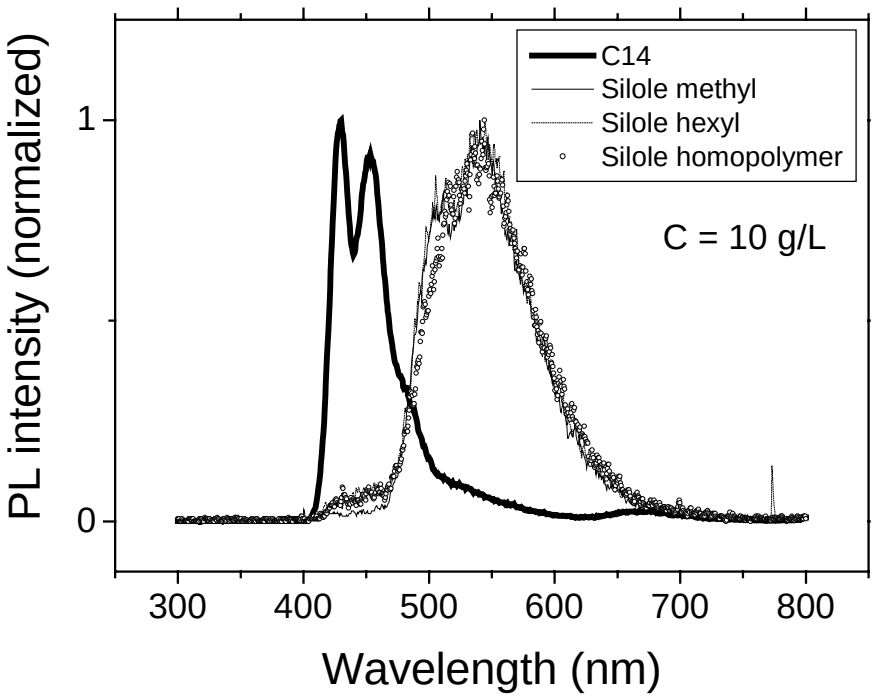
C14
Silole methyl
Silole hexyl
Silole homopolymer
C = 10 g/L
PL intensity (normalized)
1
0
300
400
500
600
700
800
Wavelength (nm)

Figure 8

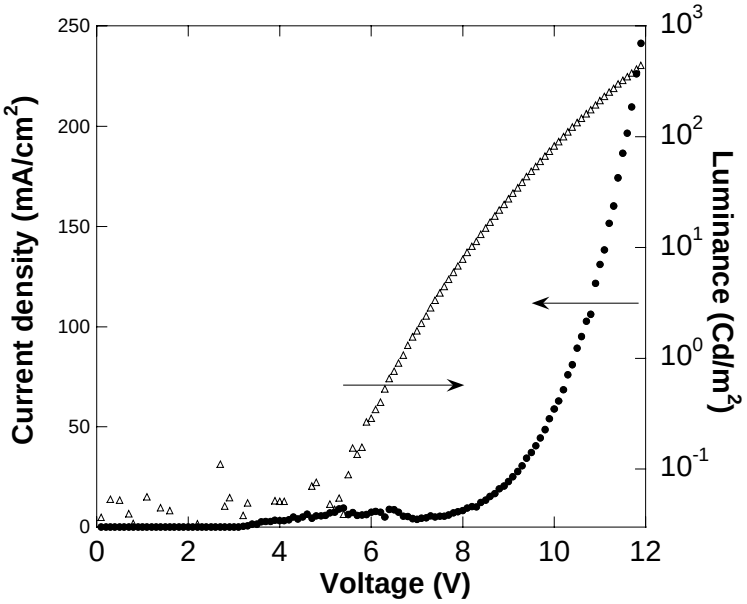
Current density (mA/cm^2)
Luminance (Cd/m^2)
Voltage (V)
0
50
100
150
200
250
0
2
4
6
8
10
12
10^{-1}
10^{0}
10^{1}
10^{2}
10^{3}

Figure 9

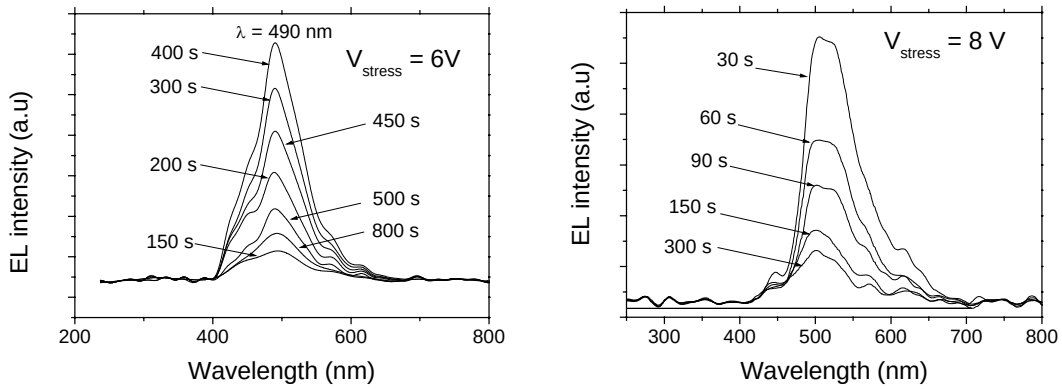
λ = 490 nm
400 s
300 s
200 s
150 s
450 s
500 s
800 s
V stress = 6V
EL intensity (a.u)
Wavelength (nm)
200
400
600
800
30 s
60 s
90 s
150 s
300 s
V stress = 8 V
EL intensity (a.u)
Wavelength (nm)
300
400
500
600
700
800

Figure 10

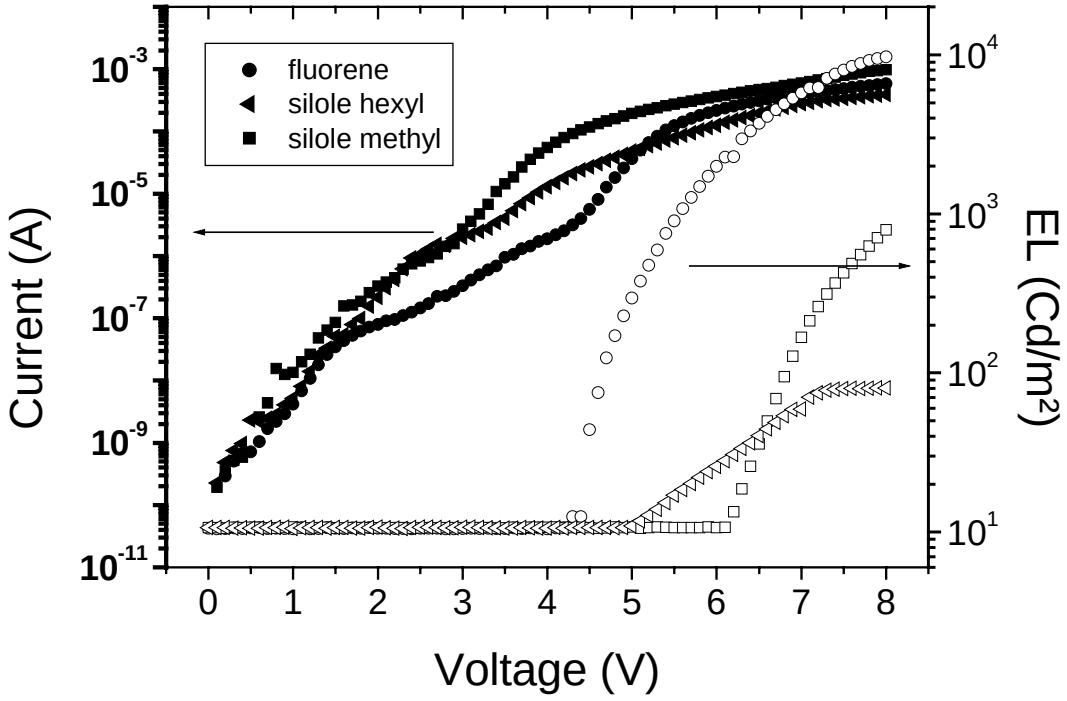
fluorene
silole hexyl
silole methyl
Current (A)
EL (Cd/m²)
Voltage (V)
10^-3
10^-5
10^-7
10^-9
10^-11
10^4
10^3
10^2
10^1
0
1
2
3
4
5
6
7
8

Figure 11

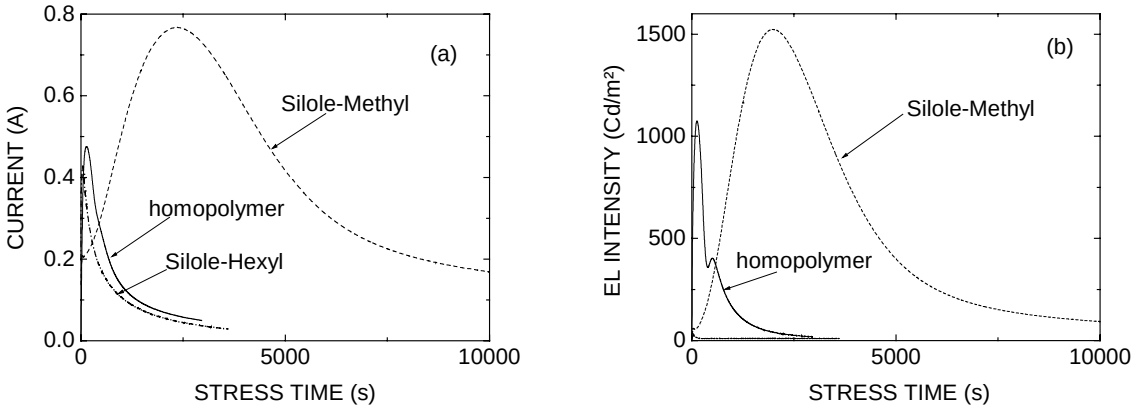
(a)
CURRENT (A)
0.0
0.2
0.4
0.6
0.8
0
5000
10000
STRESS TIME (s)
Silole-Methyl
homopolymer
Silole-Hexyl
(b)
EL INTENSITY (Cd/m²)
0
500
1000
1500
0
5000
10000
STRESS TIME (s)
Silole-Methyl
homopolymer

Figure 12

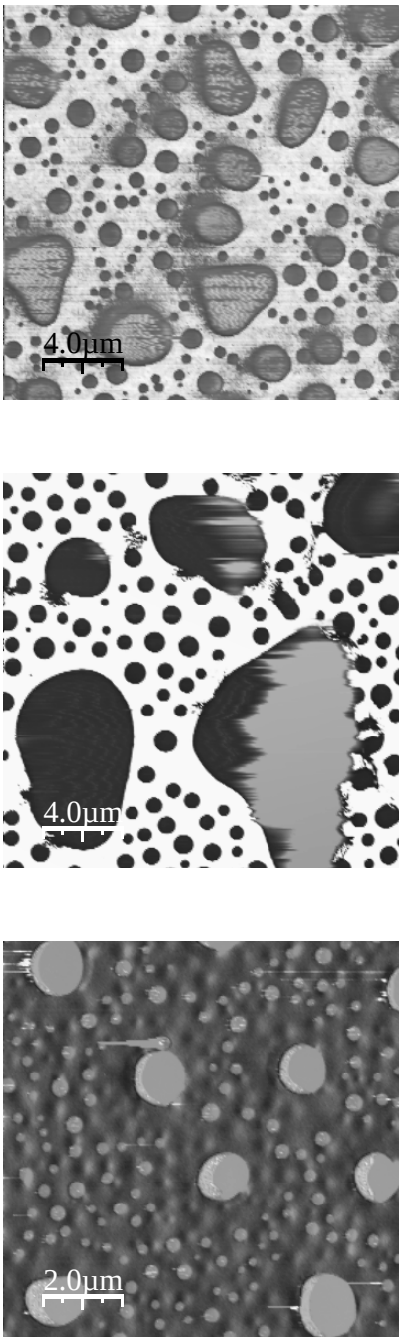

Figure 13